DOI: 10.1002/ ((please add manuscript number))
Article type: Full paper

Silver Zeolite Composites-based LEDs, a Novel Solid State Lighting Approach.

Koen Kennes, Eduardo Coutino-Gonzalez, Cristina Martin, Wouter Baekelant, Maarten Roeffaers, Mark Van der Auweraer**

Dr. K. Kennes, Dr. E. Coutino-Gonzalez, Dr. C. Martin, W. Baekelant, Prof. M. Van der Auweraer
Chem&Tech - Molecular Imaging and Photonics, KU Leuven, Celestijnenlaan 200F, B-3001 Leuven, Belgium.
Dr. E. Coutino-Gonzalez
CONACYT - Centro de Investigación y Desarrollo Tecnológico en Electroquímica, Parque Industrial Querétaro, Sanfandila s/n, Pedro Escobedo 76703, Querétaro, Mexico.
Prof. Ir. M. Roeffaers
Chem&Tech - Centre for Surface Chemistry and Catalysis, KU Leuven, Celestijnenlaan 200F, B-3001 Leuven, Belgium.

E-mail: mark.vanderauweraer@kuleuven.be, Maarten.roeffaers@kuleuven.be

Keywords: Zeolite, OLED, Electroluminescence, Silver cluster, Phosphor.

Silver clusters incorporated in a zeolite matrix represent a promising alternative for rare earth phosphors, organic dyes and quantum dots as emitters in organic and hybrid organic/inorganic light emitting diodes (OLEDs). Compared to other existing types of emitters they combine an excellent stability to oxygen and humidity with a high luminescence quantum yield and color tunability. This study reports on the first use of these silver exchanged zeolites embedded in polyvinyl carbazole (PVK), which was expected to act as a conducting matrix, as emitters in a single layer OLED. It is demonstrated that the introduction of these Ag-zeolites leads to electroluminescence bands that clearly differ from pristine PVK OLEDs as well as from the photoluminescence spectra of the Ag-zeolites. The current density and the spectral properties observed in these devices are strongly influenced by the zeolite silver loading, paving the way to a new type of easy tunable hybrid and cost effective OLEDs.

1. Introduction

The use of sub-nanometre noble metal clusters as luminescent materials has been demonstrated in the last decade.[1–7] The interest in these materials is a consequence of their peculiar physicochemical properties, resulting in intense light absorption, efficient emission and color tunability. However, the controlled synthesis and stabilization of silver clusters with well-defined sizes, shapes, and electronic properties is challenging. To overcome this problem different synthetic approaches have been proposed. Metal clusters can be stabilized by organic ligands such as small molecules[8] or organic oligomers like DNA,[9–13] acrylates,[14–17] and peptides[18] or by inorganic scaffolds like glasses.[19,20] A different approach involves a 'ship-in-a-bottle' synthesis where the growth of the metal clusters is limited by the pore size of the scaffold as for example in zeolites.[21–25] Zeolites occur as natural minerals, but can also be synthesised in industrial quantities at low cost. They are attractive as hosts for silver clusters because of the relative ease with which Ag^+ ions can be incorporated by means of cation exchange, as well as due to their well-defined crystal porosity[26] with cages and channels of (sub)molecular dimensions which can influence the geometry and nuclearity of the clusters. The wide variety of framework topologies, chemical compositions, and the possibility to introduce a wide range of extra-framework guests, such as counter-ions, make zeolites a highly versatile host/matrix system to stabilize luminescent silver species with tailored properties. Several reports have demonstrated emission from Ag-zeolites spanning the visible spectrum[2,25,27] with external quantum efficiencies approaching unity.[25,28] Therefore their use as next-generation phosphors in fluorescent lamps[29] and as wavelength converting materials in solar cells has been often suggested.[30]

Organic light emitting diodes (OLEDs) also make use of phosphors dispersed in a conductive polymer. A major drawback for commonly used emitters, both organic and inorganic, is their susceptibility to oxidation and aggregation which results in the loss of their emissive

properties.[31–33] This shortcoming is most pronounced in the case of white light OLEDs, where green emitters outlast the blue[33–35] and red[36] emitters, leading to color imbalance with time.[32,37] As the luminescent Ag clusters in zeolites are stabilized in a scaffold, preventing aggregation, they potentially offer an enhanced stability in light emitting diodes. So far, in OLEDs silver particles are either being used as electrodes[38,39] or for the electroluminescence enhancement effect caused by surface plasmon resonance.[40–42] In this work the first OLEDs where silver clusters stabilized in a zeolite framework act as active emissive structures are reported. To this purpose a single layer OLED architecture was chosen using polyvinyl carbazole (PVK) as charge transporting layer. PVK can be considered a benchmark material due to the extensive amount of research performed using this conductive polymer.[43–45] Finally, the photoluminescence (PL) and electroluminescence (EL) of these devices are studied and compared with a reference OLED.

_ENREF_13

2. Results and Discussion.

Silver exchanged zeolites with an average crystal size of ~300 nm, determined by scanning electron microscopy (SEM) **(Figure 1A)**, were prepared with a silver/sodium ratio of 6/12 (LTA[Na]-Ag_6) (*i.e.* 50% of the initial Na ions have been replaced by Ag via ion exchange). Two-dimensional (2D) excitation-emission spectra were measured to confirm the PL of the exchanged zeolites and are compiled in Figure 1B. The individual emission spectra at different excitation wavelengths can be found in **Figure SI1A**. Two main emission bands are observed; one centered around 600 nm when excited at wavelengths around 280 nm and a more intense band centered at 550 nm, with excitation maxima between 300-350 nm. Upon closer inspection, it is clear that the PL is strongly dependent on the excitation wavelength. Smaller less intense bands and/or shoulders can be observed between 425-500 nm (excitation at 375 nm), 500-600 nm and 700-800 nm (both excitations at 440 nm). The maxima of all PL bands are shown in **Table 1**. The nature of these bands have been related to differences in

silver cluster environment, geometry and nuclearity.[9] The stokes shift of the main emission band (550 nm) amounts to 12760 cm^{-1}. This large value of the Stokes shift could suggest that the electronic nature of the state absorbing at 300-350 nm is different from that of the emitting state, *i.e.* that after excitation internal conversion from the doorway state to the emitting state occurs. In order to check this possibility we calculated the Stokes shift which is expected from the fwhm of the emission using the expression $(fwhm)^2 = 16\ (\ln 2)\ E_R\ kT$,[46–48] with the Stokes shift $\Delta\bar{\nu}$ corresponding to a $2E_R$. At 290K this expression yielded starting from the observed fwhm of 3600 cm^{-1} for the main emission band a value of 11880 cm^{-1} for $\Delta\bar{\nu}$, which is close to the experimental value. Hence the emitting state has probably the same electronic nature as the doorway state that is populated by the excitation although there is a large difference in equilibrium geometry (bond lengths and bond angles inside the Ag-clusters or between the Ag-atoms and the surrounding oxygens of the zeolite framework). The external quantum yield of fluorescence of the used sample is about 33% upon excitation at 340 nm. Compared to PVK, of which the excimer has a pronounced emission maximum around 420 nm,[49] the emissive states of the Ag zeolite are situated at lower energy.

In order to further characterize the materials used for the OLEDs a 20 mg/ml solution of PVK in chlorobenzene with 10 wt% exchanged zeolites (LTA[Na]-Ag_6) with respect to PVK was spin coated on a quartz substrate to check if energy transfer from PVK to the exchanged zeolites occurs upon photo excitation of the PVK **(Figure 2)**. When exciting the sample using wavelengths between 250 nm to 350 nm, only the broad PVK emission around 420 nm was observed. Due to the excess of PVK, compared to the silver clusters in the zeolites, it is reasonable to assume that the former absorbs the majority of the light. Since we did not observe PL of the silver loaded zeolite we conclude that no efficient energy transfer occurs from PVK to the silver clusters in the zeolites. The lack of energy transfer is not a surprise since the size of the zeolite crystals is around 300 nm which means that the distance between

the large majority of the silver clusters and the polymer is much larger than typical values of the Förster distance.[50,51] Furthermore, there is little overlap between the PVK emission and the absorption of the exchanged zeolites which lead to values of the Förster distance that are significantly slower than in typical donor acceptor pairs[47,48]. To make sure that the silver exchanged zeolites are still luminescent after the sample preparation the PL of silver exchanged zeolites embedded in a in a polystyrene matrix, using the same preparation method and film thickness, was measured (Figure 2). From Figure 2 it is clear that the preparation method does not influence the PL of the exchanged zeolites.

Electroluminescence. In order to check the effect of the incorporation of silver exchanged zeolites on the electro-optical behavior of a PVK OLED, a reference OLED with an active layer of neat PVK was prepared (area: 8 mm², thickness 150 nm). **Figure 3** shows a color picture taken at 8 V, the current-voltage (IV) curve in forward bias and the EL spectrum at a driving voltage of 8 V of this reference OLED. The IV curve shows the typical behavior[52,53] of a single layer polymer light emitting diode with a turn on voltage of ~ 7 V (defined as the applied voltage where the current increases exponentially). When attempted to measure the IV curve in reversed bias the PVK layer degraded due to electron accumulation as hole injection from the low work function ytterbium becomes more difficult than electron injection from ITO. Therefore it was not possible to determine the behavior of the reference OLED under reverse bias. Under forward bias the EL of the reference OLED has a maximum at 420 nm, which corresponds to the typical PL of the full overlap excimer of PVK[44] and is stable up to an applied voltage of 20 V, after which breakdown occurs. In a following step a PVK OLED containing 10 wt% of silver exchanged zeolites, with respect to PVK, was fabricated (ZEOLED sample).

Visual inspection of the color picture of the EL of the ZEOLED (**Figure 4A**) reveals, in contrast to the picture of the homogeneous blue EL of an OLED of neat PVK an

inhomogeneous yellowish electroluminescence at 7 V. This electroluminescence becomes more intense with increasing voltage and breaks down at a bias of about 17 V (Figure 4B-C). The inhomogeneous electroluminescence suggests the presence of different discrete emissive species; this issue will be explored in more detail in the following sections. The IV curve of this ZEOLED shows a turn on voltage of 4.5 V. The EL spectra reveal, at low applied voltage, a broad emission band centered around 660 nm. Increasing the voltage yields additional features around 420, 460 and 600 nm. When performing a deconvolution (SI2) on the spectrum recorded at 15 V, 8 Gaussian bands centered at 410, 460, 510, 530, 600, 660, 720 and 820, were required to obtain a satisfying fit.

The large number of bands spanning a range from 410 to 820 nm suggests the presence of several emitting species. Combined with the spatially inhomogeneous emission (Figure 4A), considering both color and intensity this suggests that the different emitting species are not distributed homogeneously on the scale of the EL picture. The band at 410 nm corresponds with the PL band of our pristine PVK OLED and is therefore attributed to the S_1-excimer emission from PVK. This band only shows up at higher applied bias and simultaneous the bands at 460 and 600 nm appear. This suggests that at least two different injection/transport mechanisms occur and that these bands (410, 460 nm and 600 nm) are related to each other. According to literature[49,54] the bands at 460 and 600 nm can be assigned to respectively the T_1 and electromer emission bands from PVK which become pronounced in heterogeneous films of PVK. While the assignment for the 410 nm band is in line with the spectrum of the reference OLED one should note that the latter does not show the bands at 460 and 600 nm. Furthermore, for organic compounds triplet emission is seldom observed at room temperature.[55]

The deconvoluted EL spectrum shows additional bands around 510, 530, 660, 720 and 820 nm. While considering the position of the maxima some of these bands, *e.g.* the one at 720 nm, can be related to the PL (band between 700-800 nm) of the Ag-clusters, others cannot. For

those that can be related it is clear when comparing figure 2B and figure 4B or SI1 that their relative intensities are quite different. An analogous behavior was found for OLEDS with amino substituted 1,3,5-triphenylbenzenes where the EL spectra showed besides the PL spectra other maxima not present in the PL spectra and where the features of the bands present in the PL spectra have been changed in the EL spectra.[56] Assigning the EL bands to the correct PL bands is somewhat artificial due to large numbers of both PL and EL bands obtained. Upon deconvolution it can also not be excluded that defects in the zeolite framework could contribute to the EL.

To verify that these additional bands stem from the exchanged zeolites, the spatial distribution of the EL of the ZEOLED was investigated in an optical microscope (**Figure 5**). At voltages as low as 4.5 V yellowish-orange spots appeared. When the voltage was increased more of these spots emerged and around 11 V also domains with a blue-yellowish EL are observed. The latter can be ascribed to the excimer-electromer emission (410, 460 and 600 nm) originating from the polymer matrix[57] whereas the former originates from diffraction limited spots suggesting that this emission could be related to EL of silver-zeolite crystals. The colors of different spots are not uniform, ranging from yellow, orange to red, which could be related to zeolite particles with different silver loadings[58] or a non-homogeneous electric field as the function of depth or position, the latter resulting from the inhomogeneous OLED thickness. These colors also agree well with the different species obtained by the spectral deconvolution. Assuming that these spots are due to emission from exchanged zeolites and considering the lower turn on voltage, when compared to the neat PVK OLED, these data suggest that the electrons and holes are directly injected in to the zeolites at low voltages, and that the resulting current is not uniform, possibly suggesting the formation of conductive channel-like structures. At higher voltages also charge carrier injection into PVK occurs. The higher turn on voltage for the PVK EL in this ZEOLED compared to the reference OLED as well as the possible T_1 and electromer bands at 460 nm and 600 nm, can be related to the thicker and

inhomogeneous active layer in the ZEOLED structure (8 μm) compared to the pristine PVK OLED (150 nm). Attempts to make thinner layers in ZEOLEDs or thicker layers (>1μm) for the PVK OLED, in order to be able to compare both devices more accurately, were unsuccessful. Thick single layer OLEDs of neat PVK suffer from electrode breakdown before the turn on electric field is reached. Reducing the PVK concentration in the PVK/zeolite suspension results in very inhomogeneous films with unstable currents. A possible solution would be to work with mono-layers of zeolites with PVK as binder. However, we feel this should be addressed in further studies, as this is out of the scope of the present report.

Mechanism. The efficient charge carrier injection into the zeolites is quite surprising since zeolites are considered to be extremely poor conductors.[59,60] This suggests that the conduction is most likely due to the presence of silver clusters in the zeolite lattice.

In order to investigate to what extent silver clusters are involved in charge transport or injection and electroluminescence three additional zeolite batches with different Ag/Na exchange ratios (LTA[Na]-$Ag_{0.5}$, LTA[Na]-Ag_3 and LTA[Na]-Ag_{12}) were prepared and used to construct ZEOLEDs using the same procedure described earlier. In the supplementary information the 2D excitation-emission spectra of the exchanged zeolites with different Ag/Na exchange ratios are displayed (**Figure SI3**). These spectra show that the PL maximum and the features of the fluorescence spectra depend on the silver loading as reported before.[9] As expected changing the silver content also alters the EL spectra of the corresponding ZEOLEDs (**Figure SI4)**. **Figure 6A** and 6B show the IV curves of these ZEOLEDs and a plot of different ZEOLED parameters such as the maximum of the EL at 14 V, the current density at 6 V, and the voltage corresponding to an electroluminescence level of 300 counts per second, respectively, in function of the initial silver loading in the zeolite.

Interestingly, the average EL maxima show a shift to longer wavelengths upon increasing the silver loading. However, a comparison between the deconvoluted EL spectra (Figure SI2) of ZEOLED LTA[Na]-$Ag_{0.5}$ and ZEOLED LTA[Na]-Ag_6, reveals that the same emitting species are present, but with different amplitude. Figure SI2 shows that when the PVK associated bands are not taken into consideration the red emitting species become more dominant at higher silver loadings. This effect is best visible in figure 6C, which shows the CIE color coordinates of the different samples at a bias of 14 V. Changing the initial silver loading in the zeolites shifts the observed color from blue to orange-red. Although the PL of the zeolites in general undergoes a red shift with increasing Ag/Na exchange ratio, for very low exchange ratios (LTA[Na]-$Ag_{0.5}$) this is no longer the case. Table 1 shows the PL maxima of LTA[Na]-$Ag_{0.5}$ and LTA[Na]-Ag_6 and the EL maxima of the ZEOLEDs and reveals that some very distinct photoluminescent species exists in these samples although the species yielding EL are similar. This suggests the presence of weak-absorbing species in both zeolite samples which are responsible for the observed EL, most likely defects in the zeolite framework, while the strong absorbing isolated silver clusters are responsible for the PL.

A clear correlation between the current density and the silver loading is observed: higher silver loadings lead to *i)* higher current densities at the same applied voltage , *ii)* an increased intensity of the electroluminescence, *iii)* a decreased turn on voltage and *iv)* the above mentioned red shift of the EL maximum at the same applied voltage. The higher current densities and decreased turn on voltage reveal that a significant part of the minority carriers are injected and transported through the silver clusters and that at least a significant part of the current flows through the clusters in the zeolites with a mobility that is higher than the corresponding charge mobility in pure PVK.

Figure 7A shows the energy levels of the materials used. Both the LUMO of the used zeolite framework[62-63] and PVK match with the work function of the Yb cathode. Therefore electron injection in both of them is in principle possible. Holes can efficiently be injected from ITO into PVK,[61] however, it is unlikely that they are injected into the HOMO of the zeolite framework due to the large energy difference. According to literature the band gap of small clusters fits well within the zeolite framework bandgap.[62,63] Although the exact bandgap is still unknown, the Fermi level of the silver clusters was determined at ~5.1 eV via UV impact spectroscopy,[28] meaning that their bandgap also fits within that of PVK. These energetic features suggest that efficient hole injection from ITO can occur into PVK as well as directly into the clusters. Electrons can be injected into PVK, the zeolite LUMO and into the clusters. Due to the smaller bandgap the clusters can act as a trap where either recombination occurs or from where the charges escape either via transfer to PVK (energetically less likely) or via hopping to neighboring clusters both inter and intra-zeolite.

Charge transport through the devices can occur by different mechanisms as depicted in figure 7B. Case i) a channel formed by the silver clusters in the zeolites embedded in the PVK matrix acts as a conductive pathway for holes and/or electrons hopping between the silver clusters (inter or intrazeolite). Case ii) shows a combination of electron injection into a silver cluster inside a zeolite crystal in contact with the cathode and hole injection into PVK. The injected electrons can either stay in the cluster in which they are initially injected or hop between different clusters to the opposite side of the zeolite crystal where they in first instance get trapped. At sufficiently high fields they can get injected in the LUMO of the PVK matrix and hop in the PVK matrix until they get trapped by a silver cluster in another zeolite crystal. Eventually they recombine with holes injected in the PVK matrix that get trapped by the silver clusters in the zeolite. Case iii) corresponds to electron injection into PVK followed by trapping in the silver clusters in the zeolite. The lower observed turn on voltage of the EL (4.5V) in the ZEOLED compared to an OLED of neat PVK and the fact that upon increasing

the applied voltage silver zeolite emission is observed before PVK emission suggests that mechanism i) is more relevant than mechanisms ii) and iii). In either of these mechanisms charge carrier transport between different silver clusters is vital. This does not mean that all clusters should form larger aggregates which are non-luminescent. Non-coherent charge carrier transport by electron or hole transfer between two neighboring clusters will already occur at distances that can be up to 1 or 2 nm. At these distances, where the electron transfer is non-adiabatic, the electronic coupling between two neighboring clusters will be too small to result in a delocalized wavefunction and the corresponding loss of fluorescence. A similar mechanism was recently proposed for metal organic frameworks (MOFs), where a (photo)conduction increment of about 4 orders of magnitude could be achieved due to the inclusion of 1.4 v% silver particles with an average separation distance up to 2 nm.[64]

The observed results can be rationalized if one assumes that the photoluminescence is mainly due to isolated silver clusters (separation distance > 2 nm). Although strongly interacting silver clusters which behave as conductive channels show poor luminescent properties they can be involved in the transport of charges to luminescent defect centers in the zeolite framework itself. A higher silver loading can then enhance the amount of conductive pathways and increase the contribution of the EL of the red emitting species. A limiting factor for a further elucidation of the complex nature of the injection/conduction mechanism and the exact nature of the EL is the use of the conductive PVK matrix. Besides complicating the EL spectra of the silver doped zeolite crystals by intrinsic PVK emission, the lower stability of this matrix, especially under reverse bias, prohibits a large range of device modifications. In a follow up study PVK will be replaced by a non-conductive and non-emissive polymer in order to obtain more insights in the conductive and electroluminescent properties of these novel ZEOLEDs.

3. Conclusions

Introducing luminescent silver exchanged zeolites as emitters in a conductive polymer matrix leads to new electroluminescence bands which can be linked to the zeolites and hence to a new class of LEDs; the ZEOLEDs. Although the electroluminescence bands differ from the photoluminescence bands, the CIE coordinates of these ZEOLEDs could be fine-tuned from blue to red and even achieve near white light (CIE: x: 0.32, y: 0.35) by changing the silver concentration in the zeolite framework. The dependence of the current on the silver loading suggests that charge injection and transport occur directly through the silver exchanged zeolites. Therefore it is probably not necessary to use a conductive matrix such as PVK in the fabrication of the ZEOLED. Hence further research on the ZEOLEDs should focus on the injection and transport mechanism in these devices using a non-conductive and non-emissive matrix instead of PVK. The ZEOLEDs allow to obtain a tunable emission using abundant and easily processed zeolites as charge transport and emitting material. As the organic matrix only plays a minor role one can also expect that the instability inherent to charge transport through and excitation of organic molecules will no longer limit the lifetime of the ZEOLEDs.

4. Experimental Section

Synthesis of silver exchanged zeolites: Commercial zeolites, from Nanoscope, with a crystal size distribution of around ~300 nm were used. The zeolites were exchanged with Ag cations following the procedure described in detail elsewhere.[9] Briefly, 500 mg of zeolite powder were suspended in an aqueous silver nitrate solution (500 mL, 0.04 - to 0.5 mM, Sigma-Aldrich, 99% purity), then the suspension was stirred for 2 hours in the dark. The powder was recovered by filtration using a Büchner filter and washed several times with milliQ water, then the sample was calcined overnight at 450 °C (5 °C min^{-1}) preceded by 2 steps of 15 minutes each at 100 and 150 °C to prevent any damage in the zeolite structure during the calcination process. After the heat treatment the sample was cooled under ambient conditions and stored in the dark for further analysis. The structural formula for the fully dehydrated

LTA zeolites, after normalization of the total amount of T atoms in the unit cell to 24, is $(M_{12}^{+})[Si_{12}Al_{12}O_{48}]$ where M represents the counter-balancing ion. The amount of silver cations that can be exchanged in LTA zeolites ranges from 1 to 12 per normalized unit cell; we therefore prepared samples containing low, intermediate and high silver loadings to study the effect of the silver content on their electroluminescence properties. We denoted the samples as follows; LTA[M]-Ag_x, where M represents the charge balancing counter-ion in the zeolite and *x* represents the amount of silver atoms per normalized unit cell (1-12).

Device fabrication: A solution of PVK (Sigma Aldrich: Mn~25.000-50.000 $g.mol^{-1}$) in chlorobenzene (20 mg/ml), with or without 10 wt% of silver exchanged zeolites with respect to PVK, was spin coated at 1000 rpm for 60 seconds on an ultrasonically cleaned and ozone treated ITO substrate. Next, a 100 nm Ytterbium electrode was vapor deposited on top of the PVK layer. Ytterbium was chosen for its low work function and higher stability to oxygen compared to other low work function metals like alkaline earth metals (Ca, Mg,). In order to obtain a good dispersion, the suspension was sonicated at 45 °C for 2.5 hours prior to spin coating (1000 rpm, 60 s). In the supporting information the importance of this sonication step is explained.

Stationary fluorescence measurements. Measurements were recorded using a fluorimeter (Edinburgh fls980). The spectrometer was corrected for the wavelength dependence of the throughput of the emission monochromator and the sensitivity of the detector. The external quantum yield of luminescence is defined as the quantum yield of fluorescence of the silver exchanged zeolites and might be lower than the quantum yield of fluorescence of the individual silver clusters and was determined using an integrating sphere following the report described elsewhere.[7b]

Stationary electroluminescence measurements. Stationary measurements have been recorded using a nitrogen cooled CCD (Princeton Instruments SPEC-10:100B/LN eXcelen CCD camera, SP 2356 spectrometer with 1-030-500 grating 300 g/mm @ 500 nm).

IV-curves.

All IV-curves were measured in the dark at room temperature using a Keihtley 2400 device.

Scanning electron microscope (SEM) measurements.

SEM measurements were performed on a SEM JEOL JSM-6010LV microscope using the InTouch Scope software.

Supporting Information
Supporting Information is available from the Wiley Online Library or from the author.

Acknowledgements

K. Kennes is funded by a personal PhD grant from the Agency for Innovation, Science and Technology (IWT) Flanders. The authors are also indebted to Belspo program through IAP VI/27 and VII/05 and to the KULeuven Research Fund through GOA 2011/3 and C14/15/053. The authors gratefully acknowledge financial support from the European Union's Seventh Framework Programme (FP7/2007-2013 under grant agreement no. 310651 SACS). We thank E. De Keyzer and B. Dieu for their assistance in producing the Ag-zeolite samples and graphical material.

Received: ((will be filled in by the editorial staff))
Revised: ((will be filled in by the editorial staff))
Published online: ((will be filled in by the editorial staff))

[1] S. Choi, R. M. Dickson, J. Yu, *Chem. Soc. Rev.* **2012**, *41*, 1867.
[2] I. Díez, R. H. a Ras, *Nanoscale* **2011**, *3*, 1963.
[3] S. Bhandari, S. Pramanik, R. Khandelia, A. Chattopadhyay, *ACS Appl. Mater. Interfaces* **2016**, *8*, 1600.
[4] M. C. Alonso, L. Trapiella-Alfonso, J. M. C. Fernández, R. Pereiro, A. Sanz-Medel, *Biosens. Bioelectron.* **2016**, *77*, 1055.
[5] B. Rodríguez-González, A. Burrows, M. Watanabe, C. J. Kiely, L. M. Liz Marzán, *J. Mater. Chem.* **2005**, *15*, 1755.
[6] W. Wu, D. Yu, H.-A. Ye, Y. Gao, Q. Chang, *Nanoscale Res. Lett.* **2012**, *7*, 301.
[7] L. Shang, S. Dong, G. U. Nienhaus, *Nano Today* **2011**, *6*, 401.

[8] J. Zheng, R. M. Dickson, *J. Am. Chem. Soc.* **2002**, *124*, 13982.
[9] T. Vosch, Y. Antoku, J.-C. Hsiang, C. I. Richards, J. I. Gonzalez, R. M. Dickson, *Proc. Natl. Acad. Sci. U. S. A.* **2007**, *104*, 12616.
[10] M. R. Carro Temboury, V. Paolucci, E. N. Hooley, L. Latterini, T. Vosch, *Analyst* **2016**, *141*, 123.
[11] P. Shah, A. Rørvig-Lund, S. Ben Chaabane, P. W. Thulstrup, H. G. Kjaergaard, E. Fron, J. Hofkens, S. W. Yang, T. Vosch, *ACS Nano* **2012**, *6*, 8803.
[12] D. Schultz, K. Gardner, S. S. R. Oemrawsingh, N. Markesevic, K. Olsson, M. Debord, D. Bouwmeester, E. Gwinn, *Adv. Mater.* **2013**, *25*, 2797.
[13] S. M. Copp, P. Bogdanov, M. Debord, A. Singh, E. Gwinn, *Adv. Mater.* **2014**, *26*, 5839.
[14] P. Kunwar, J. Hassinen, G. Bautista, R. H. A. Ras, J. Toivonen, A. Physics, **2014**, 11165.
[15] I. Díez, M. Pusa, S. Kulmala, H. Jiang, A. Walther, A. S. Goldmann, A. H. E. Müller, O. Ikkala, R. H. A. Ras, *Angew. Chemie - Int. Ed.* **2009**, *48*, 2122.
[16] J. Zhang, S. Xu, E. Kumacheva, *Adv. Mater.* **2005**, *17*, 2336.
[17] B. G. Ershov, A. Henglein, *J. Phys. Chem. B* **1998**, *102*, 10667.
[18] J. Yu, S. A. Patel, R. M. Dickson, *Angew. Chemie - Int. Ed.* **2007**, *46*, 2028.
[19] Y. Watanabe, G. Namikawa, T. Onuki, K. Nishio, T. Tsuchiya, *Appl. Phys. Lett.* **2001**, *78*, 2125.
[20] A. Royon, K. Bourhis, M. Bellec, G. Papon, B. Bousquet, Y. Deshayes, T. Cardinal, L. Canioni, *Adv. Mater.* **2010**, *22*, 5282.
[21] G. Calzaferri, C. Leiggener, S. Glaus, D. Schürch, K. Kuge, *Chem. Soc. Rev.* **2003**, *32*, 29.
[22] G. De Cremer, E. Coutiño-Gonzalez, M. B. J. Roeffaers, D. E. De Vos, J. Hofkens, T. Vosch, B. F. Sels, *ChemPhysChem* **2010**, *11*, 1627.
[23] E. Coutino-Gonzalez, D. Grandjean, M. Roeffaers, K. Kvashnina, E. Fron, B. Dieu, G. De Cremer, P. Lievens, B. Sels, J. Hofkens, *Chem. Commun.* **2014**, *50*, 1350.
[24] G. De Cremer, B. F. Sels, J. I. Hotta, M. B. J. Roeffaers, E. Bartholomeeusen, E. Coutiño-Gonzalez, V. Valtchev, D. E. De Vos, T. Vosch, J. Hofkens, *Adv. Mater.* **2010**, *22*, 957.
[25] E. Coutino-Gonzalez, M. B. J. Roeffaers, B. Dieu, G. De Cremer, S. Leyre, P. Hanselaer, W. Fyen, B. Sels, J. Hofkens, *J. Phys. Chem. C* **2013**, *117*, 6998.
[26] C. J. Van Oers, M. Kurttepeli, M. Mertens, S. Bals, V. Meynen, P. Cool, *Microporous Mesoporous Mater.* **2014**, *185*, 204.
[27] G. De Cremer, E. Coutiño-Gonzalez, M. B. J. Roeffaers, B. Moens, J. Ollevier, M. Van der Auweraer, R. Schoonheydt, P. a Jacobs, F. C. De Schryver, J. Hofkens, D. E. De Vos, B. F. Sels, T. Vosch, *J. Am. Chem. Soc.* **2009**, *131*, 3049.
[28] O. Fenwick, E. Coutino-Gonzalez, D. Grandjean, W. Baekelant, F. Richard, S. Bonacchi, D. De Vos, P. Lievens, M. Roeffaers, J. Hofkens, P. Samori, *Nat. Mater.* **2016**.
[29] T. Vosch, B. F. Sels, M. B. J. Roeffaers, J. Hofkens, D. E. De Vos, G. De Cremer, BE2008/0050 (WO 2009006707) **2009**.
[30] T. Vosch, B. F. Sels, M. B. J. Roeffaers, J. Hofkens, D. E. De Vos, G. De Cremer, BE2008/0051 (WO 2009006707) **2009**.
[31] G. Schwabegger, T. Dingemans, R. Resel, H. Sitter, C. Simbrunner, *Appl. Phys. A* **2014**, *115*, 731.
[32] S. Yang, M. Jiang, *Chem. Phys. Lett.* **2009**, *484*, 54.
[33] C. G. Zhen, Y. F. Dai, W. J. Zeng, Z. Ma, Z. K. Chen, J. Kieffer, *Adv. Funct. Mater.* **2011**, *21*, 699.
[34] H. Sasabe, J. Kido, *Chem. Mater.* **2011**, *23*, 621.
[35] M. Zhu, C. Yang, *Chem. Soc. Rev.* **2013**, *42*, 4963.

[36] G. Tregnago, C. Fléchon, S. Choudhary, C. Gozalvez, A. Mateo-Alonso, F. Cacialli, *Appl. Phys. Lett.* **2014**, *105*.
[37] H. T. Nicolai, A. Hof, P. W. M. Blom, *Adv. Funct. Mater.* **2012**, *22*, 2040.
[38] H. Kermani, H. R. Fallah, M. Hajimahmoodzadeh, N. Basri, *Thin Solid Films* **2013**, *539*, 222.
[39] S. J. Lee, Y.-H. Kim, J. K. Kim, H. Baik, J. H. Park, J. Lee, J. Nam, J. H. Park, T.-W. Lee, G.-R. Yi, J. H. Cho, *Nanoscale* **2014**, *6*, 11828.
[40] C.-Y. Gao, Y.-C. Chen, K.-L. Chen, C.-J. Huang, *Appl. Surf. Sci.* **2015**, *359*, 749.
[41] S. Khadir, M. Chakaroun, A. Belkhir, A. Fischer, O. Lamrous, A. Boudrioua, *Opt. Express* **2015**, *23*, 23647.
[42] W. Zhang, Y. Chen, L. Gan, J. Qing, X. Zhou, Y. Huang, Y. Yang, Y. Zhang, J. Ou, X. Chen, M. Qiu Zhang, *J. Phys. Chem. Solids* **2014**, *75*, 1340.
[43] S. Ambrozevich, M. van der Auweraer, D. Dirin, M. Parshin, R. Vasil'ev, A. Vitukhnovsky, *J. Russ. Laser Res.* **2008**, *29*, 526.
[44] A. Khetubol, Y. Firdaus, a. Hassinen, S. Van Snick, Z. Hens, W. Dehaen, M. Van der Auweraer, **2012**, *8424*, 84242W.
[45] I. G. Scheblykin, L. S. Lepnev, a. G. Vitukhnovsky, M. Van der Auweraer, *J. Lumin.* **2001**, *94–95*, 461.
[46] G. Verbeek, S. Depaemelaere, M. Van der Auweraer, F. C. De Schryver, A. Vaes, D. Terrell, S. De Meutter, *Chem. Phys.* **1993**, *176*, 195.
[47] M. A. Marcus, *J. Chem. Phys.* **1965**, *43*, 1261.
[48] B. S. Brunschwig, S. Ehrenson, N. Sutin, *J. Phys. Chem.* **1987**, *91*, 4714.
[49] T. Ye, J. Chen, D. Ma, *Phys. Chem. Chem. Phys.* **2010**, *12*, 15410.
[50] F. C. De Schryver, T. Vosch, M. Cotlet, M. Van der Auweraer, K. Müllen, J. Hofkens, *Acc. Chem. Res.* **2005**, *38*, 514.
[51] M. Cotlet, T. Vosch, S. Habuchi, T. Weil, K. Müllen, J. Hofkens, F. De Schryver, *J. Am. Chem. Soc.* **2005**, *127*, 9760.
[52] H. A. Méndez-pinzón, D. R. Pardo-pardo, J. P. Cuéllar-alvarado, J. Carlos, R. Vera, B. A. Páez-sierra, **2010**, *15*, 68.
[53] P. D'Angelo, M. Barra, a. Cassinese, M. G. Maglione, P. Vacca, C. Minarini, a. Rubino, *Solid. State. Electron.* **2007**, *51*, 123.
[54] C. C. Yap, M. Yahaya, M. M. Salleh, *Curr. Appl. Phys.* **2009**, *9*, 1038.
[55] N. J. Turro, *Modern molecular photochemistry*; University Science books, 1991.
[56] J. Rommens, A. Vaes, M. Van der Auweraer, F. C. De Schryver, H. Bässler, H. Vestweber, J. Pommerehne, *J. Appl.Phys.,* **1998**, *84*, 4487.
[57] I. Glowacki, Z. Szamel, *J. Phys. D. Appl. Phys.* **2010**, *43*, 295101.
[58] E. Coutino-Gonzalez, W. Baekelant, D. Grandjean, M. B. J. Roeffaers, E. Fron, M. S. Aghakhani, N. Bovet, M. Van der Auweraer, P. Lievens, T. Vosch, B. Sels, J. Hofkens, *J. Mater. Chem. C* **2015**, *3*, 11857.
[59] V. I. Orbukh, N. N. Lebedeva, S. Ozturk, B. G. Salamov, *Superlattices Microstruct.* **2013**, *54*, 16.
[60] M. Álvaro, J. F. Cabeza, D. Fabuel, A. Corma, H. García, *Chem. - A Eur. J.* **2007**, *13*, 3733.
[61] A. Khetubol, A. Hassinen, Y. Firdaus, W. Vanderlinden, S. Van Snick, S. Flamée, B. Li, S. De Feyter, Z. Hens, W. Dehaen, M. Van Der Auweraer, *J. Appl. Phys.* **2013**, *114*.
[62] R. Seifert, R. Rytz, G. Calzaferri, *Society* **2000**, 7473.
[63] D. Bru, R. Seifert, G. Calzaferri, *Exposure* **1999**, *103*, 7.
[64] S. Han, S. C. Warren, S. M. Yoon, C. D. Malliakas, X. Hou, Y. Wei, M. G. Kanatzidis, B. a. Grzybowski, *J. Am. Chem. Soc.* **2015**, *137*, 8169.

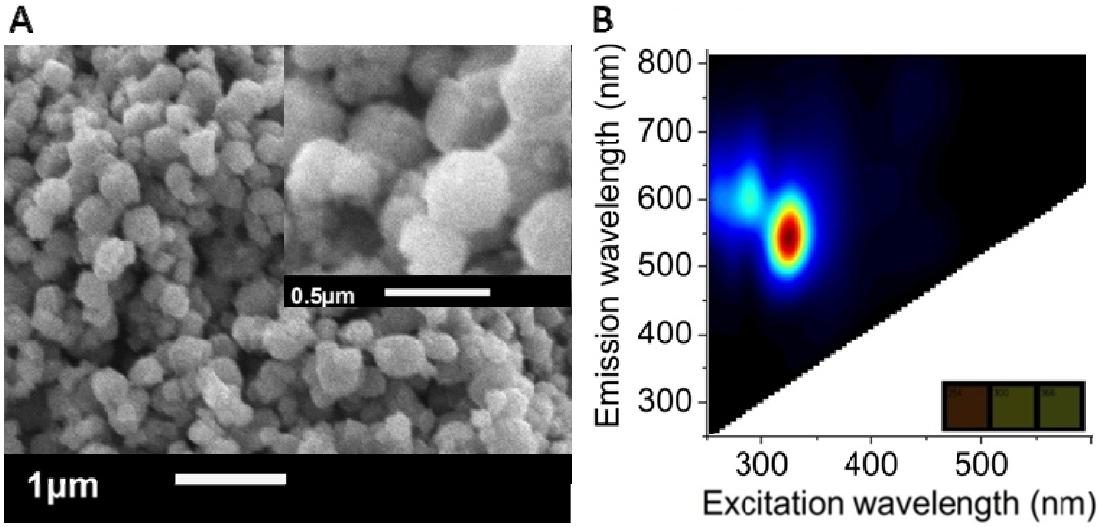

Figure 1. A) SEM micrograph image of the zeolites used in this report. The micrograph shows zeolite crystals with sizes around 300 nm. (B) Normalized 2D excitation-emission plot of the silver exchanged zeolite powder (LTA[Na]-Ag_6).

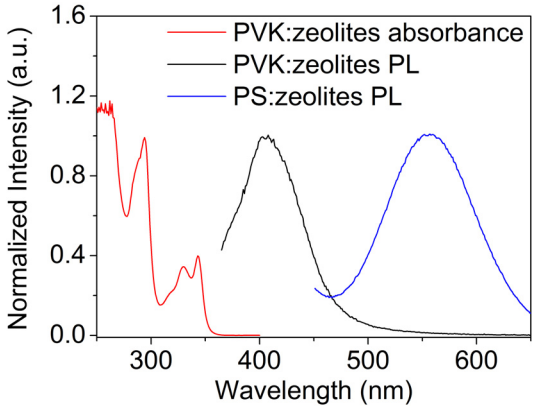

Figure 2. Absorption and PL of the silver exchanged zeolite (LTA[Na]-Ag_6) embedded in a PVK matrix (ZEOLED) and PL of the silver exchanged zeolite in a PS matrix. Excitation occurred at 350 nm and the spectra are normalized to one at the maximum.

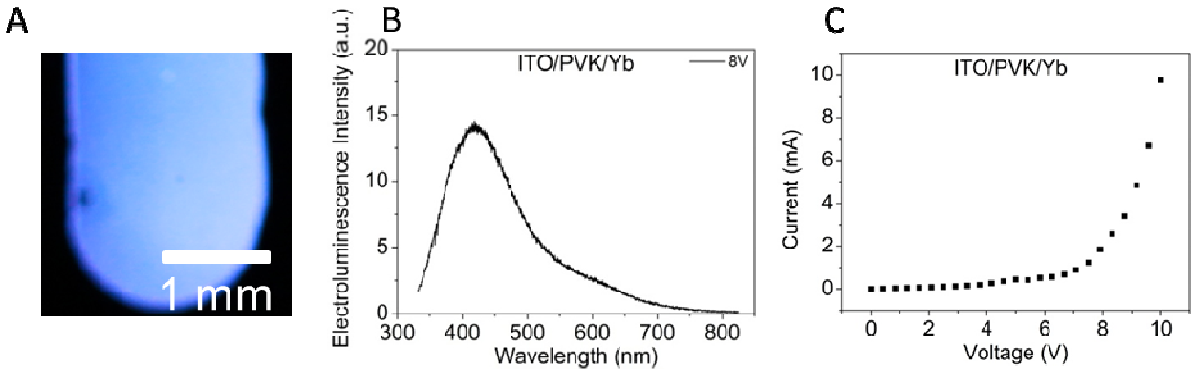

Figure 3. (A) Micrograph of a reference PVK OLED at 8 V bias, (B) EL spectrum at 8V bias and (C) IV curve.

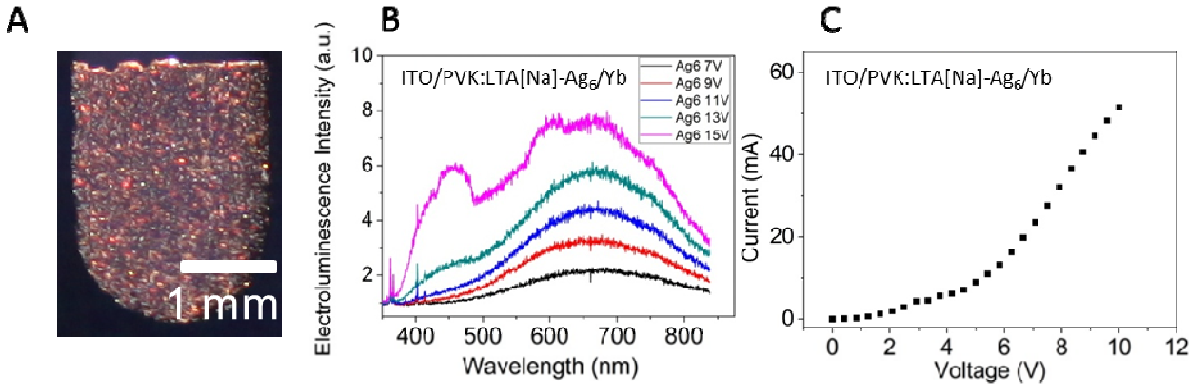

Figure 4. (A) Color picture of a working ZEOLED (PVK + 10 wt% zeolite (LTA[Na]-Ag_6) at 7 V bias), (B) Electroluminescence spectra, (C) IV curve.

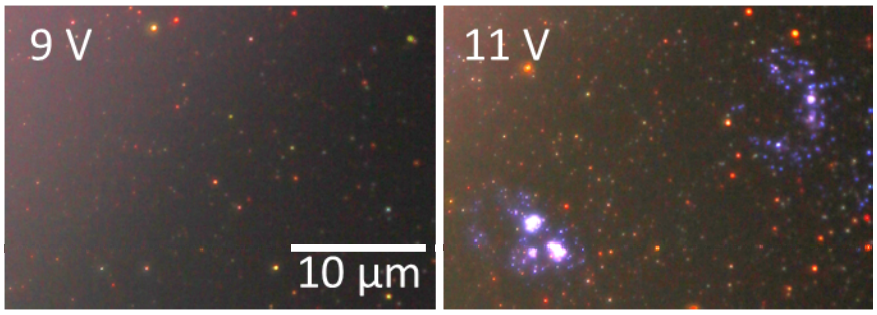

Figure 5. EL of a ZEOLED, PVK + 10 w% zeolite (LTA[Na]-Ag_6, observed under an optical microscope (60X).

LTA[Na]-Ag_6 PL maxima (nm)	LTA[Na]-$Ag_{0.5}$ PL maxima (nm)	Deconvoluted EL maxima (nm)
	374	
		410
460	446	460
		510

550	553	530
610		600
	650	660
740		720
		820

Table 1. Deconvoluted PL maxima of LTA[Na]-Ag_6 and LTA[Na]-$Ag_{0.5}$ and the EL maxima of the respective ZEOLEDs.

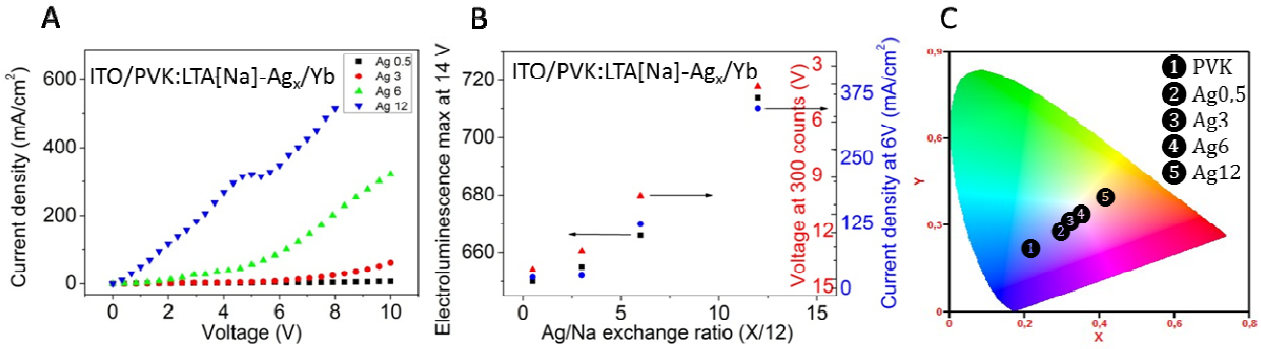

Figure 6. A) IV curves of ZEOLEDs with different silver loadings (LTA[Na]-$Ag_{0.5/12,\ 3/12,\ 6/12}$). B) Electroluminescence maximum at 14 V, emission intensity (expressed as the voltage required to obtain a level of 300 photon counts per second) and current density at 6V in function of the initial silver loading. C) CIE coordinates of the EL at 14 V.

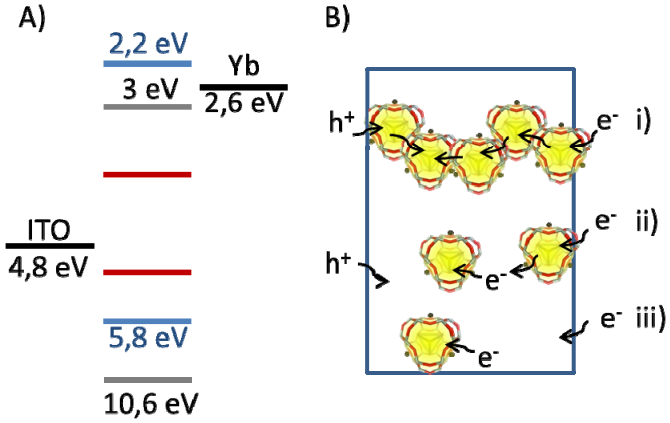

Figure 7. (A) Energy levels of the materials used. PVK: blue,[61] zeolite: gray,[63] silver species: red.[28] (B) Scheme of possible charge injection and transport mechanisms; i) a conductive zeolite pathway, ii) & iii) injection in either the exchanged zeolite or PVK and charge exchange between them.

The table of contents entry should be 50–60 words long,

The development of innovative, efficient and cost-effective lighting sources is nowadays of paramount importance. Here we describe for the first time the assembly and characterization of silver exchanged zeolite-based LEDs. We employ a basic, single layer OLED architecture in which silver exchanged zeolites are incorporated. The electroluminescence colors are controlled by the silver concentration in the zeolites.

Keyword
Ag-zeolite electroluminescence

Mark van der Auweraer*

Title Silver Zeolite Composites-based LEDs, a Novel Solid State Lighting Approach.

ToC Figure ((Please choose one size: 55 mm broad × 50 mm high **or** 110 mm broad × 20 mm high. Please do not use any other dimensions))

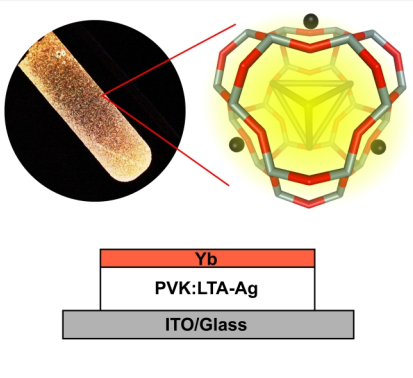

Supporting Information

Silver zeolite composites-based LEDs, a novel solid state lighting approach.

Koen Kennes, Eduardo Coutino-Gonzalez, Cristina Martin, Wouter Baekelant, Maarten Roeffaers, Mark Van der Auweraer**

*Corresponding author

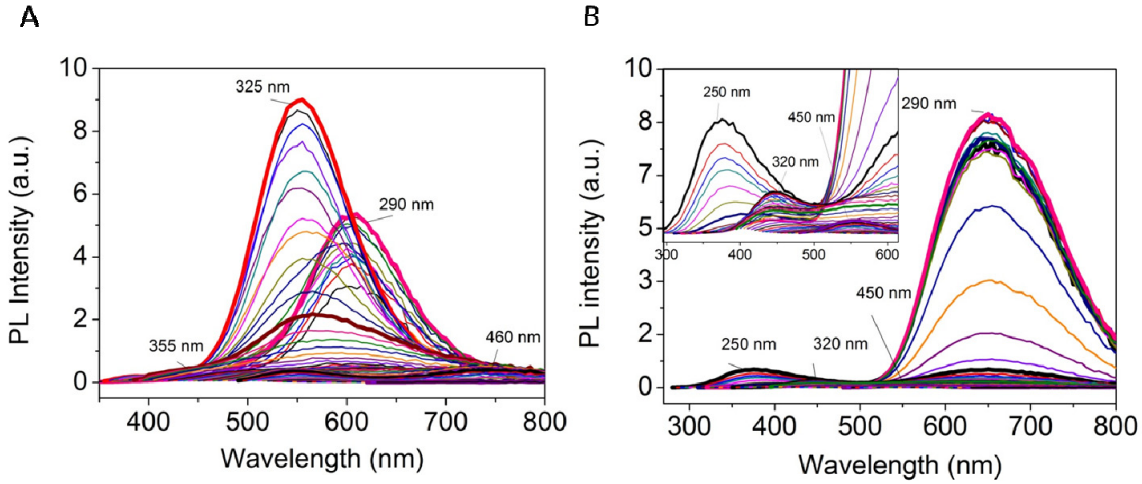

Figure SI1. PL spectra of zeolite power. A) LTA[Na]-Ag_6 and B) LTA[Na]-$Ag_{0.5}$. The indicated wavelengths are the excitation wavelengths where the specific PL band reaches maximum intensity.

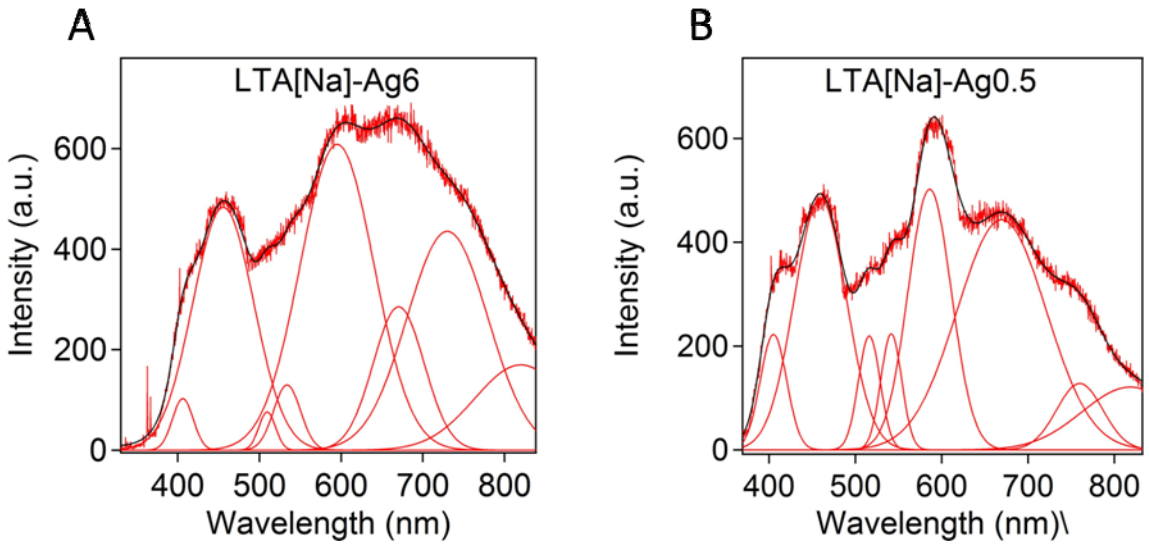

Figure SI2. Deconvoluted EL spectrum of two; (A) a LTA[Na]-Ag_6 ZEOLED at 15V and (B) a LTA[Na]-$Ag_{0.5}$ ZEOLED at 16V.

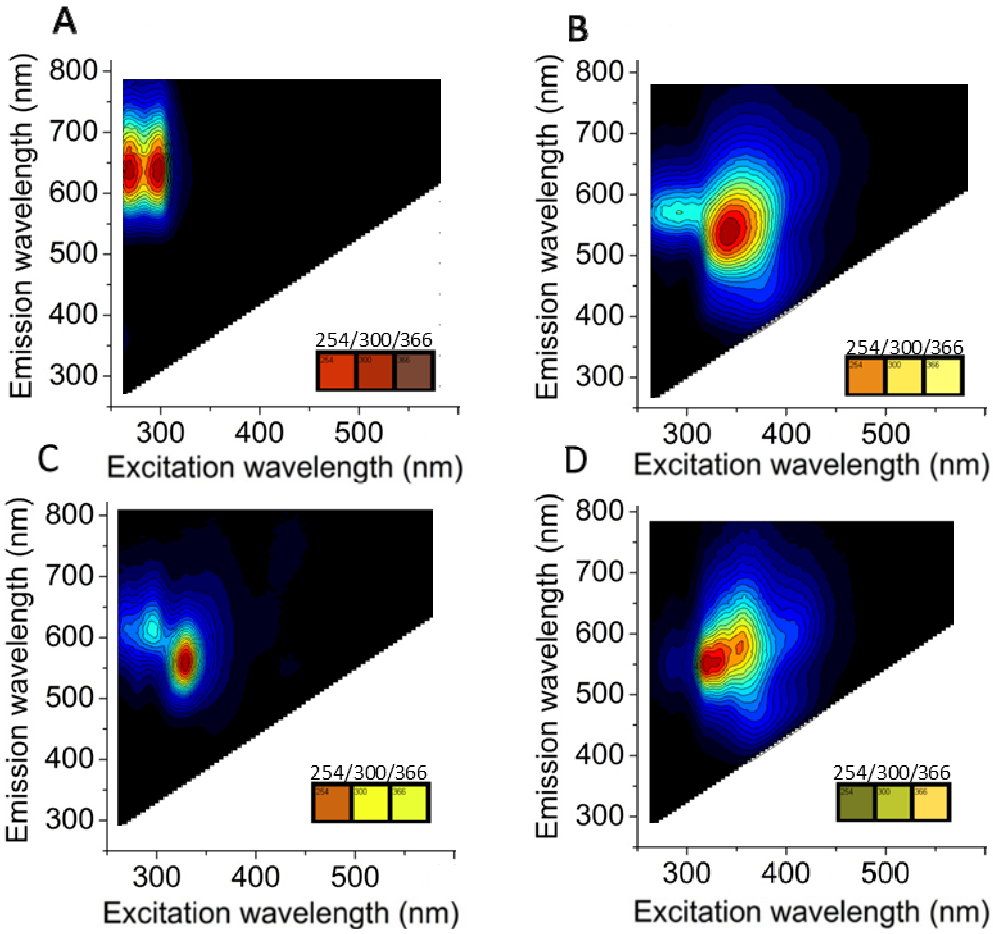

Figure SI3. 2D excitation-emission plots for silver exchanged zeolites with different silver loadings; the silver/sodium exchange ratio amounted to: A) LTA[Na]-$Ag_{0.5}$, B) LTA[Na]-Ag_3, C) LTA[Na]-Ag_6, and D) LTA[Na]-Ag_{12}. The insets display the simulated emission colors of the samples at the indicated excitation wavelengths based on the information collected from the 2D plots.

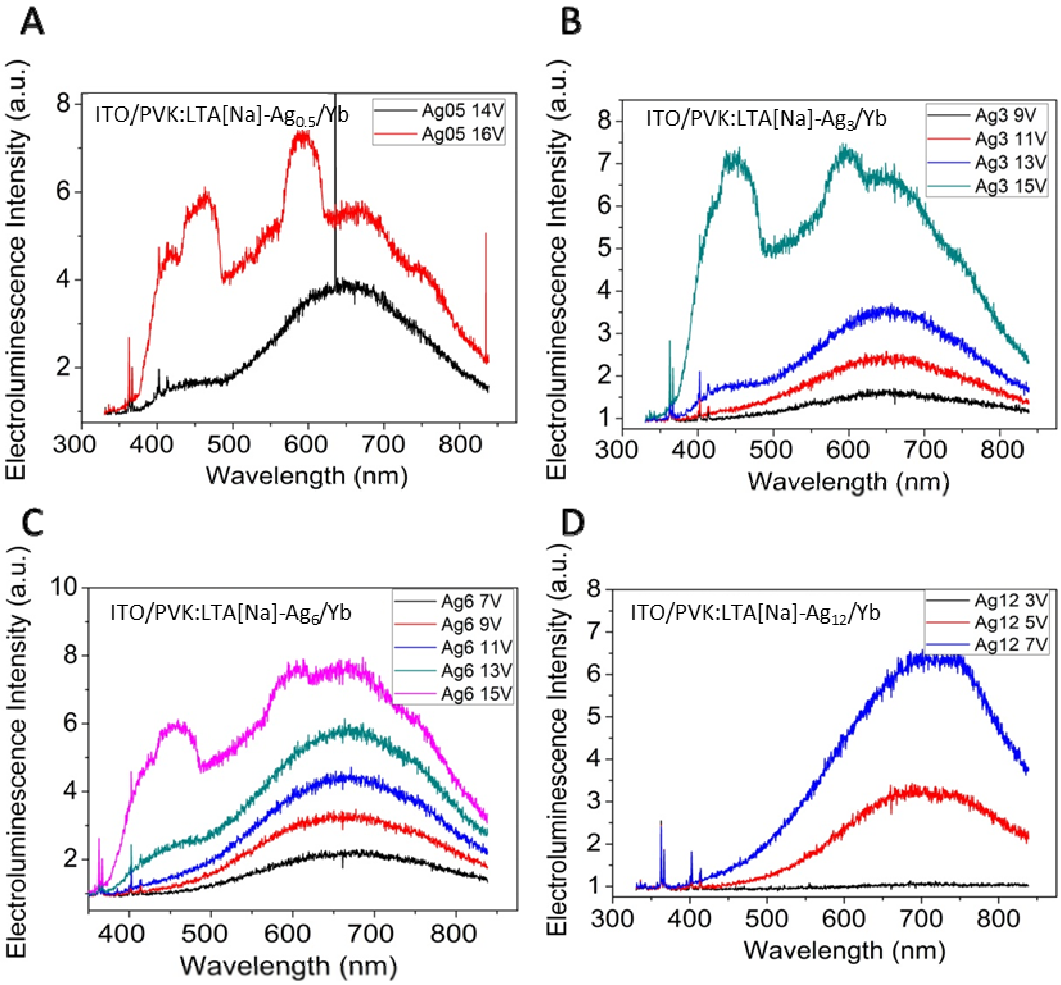

Figure SI4. Applied voltage dependence of the electroluminescence spectra of ZEOLEDs with different silver/sodium exchange ratios of respectively: A) LTA[Na]-$Ag_{0.5}$, B) LTA[Na]-Ag_3, C) LTA[Na]-Ag_6, and D) LTA[Na]-Ag_{12}.

Influence of sonication of the spin coating solution on the properties of the ZEOLEDs.

To obtain a better and more homogenous Ag-zeolite suspension the use of sonication is of vital importance. This will have a pronounced effect on the morphology of the polymer film after spin coating. Without a good contact between the zeolites and PVK, charges will not be transported between the zeolite crystals, but rather accumulate on their surface leading to EL of PVK electromers. Electromers are formed in the solid state when two molecules with charge carriers with opposite charge interact in their excited states.[1] The formation of electromers can be enhanced by trapping of the carriers at the electromer site or when transport is limited. Instead of recombining on one emissive center a new excited state similar to an excimer, where the excitation is delocalized over two neighboring chromophores is formed. This state yields emission with a very pronounced bathochromic shift. In **Figure SI5** the EL spectra of such a device, fabricated without sonication of the spin coating solution, are

shown. Besides the typical PVK band at 420 nm an electromer band at 610 nm is observed. Increasing the driving voltage should favor the electromer emission compared to the emission from the other species due to the higher charge carrier density in the PVK matrix. From the inset of Figure SI5 it is clear that the ratio of electromer intensity versus PVK excimer intensity increases with increasing driving voltage. More information about possible electromer emission in PVK can be found elsewhere.[1] The sonication process breaks up agglomerated zeolites and ensures a more homogeneous distribution of the zeolites in the polymer solution. This will result in a more homogeneous film after spin coating leading to better charge transport through the silver exchanged zeolites and less electromer emission.

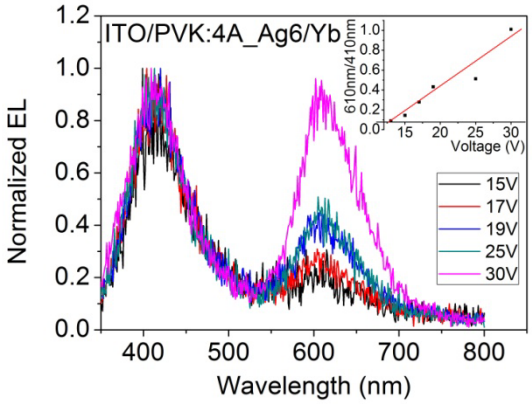

Figure SI5. EL of a ZEOLED fabricated without the sonication step. In this particular device zeolites of 2µm in size were used although smaller zeolites give similar results.

[1] C. C. Yap, M. Yahaya, M. M. Salleh, *Curr. Appl Phys.* **2009**, *9*, 1038-1041.